Optoacoustic imaging of an animal model of prostate cancer

Michelle P. Patterson[1,2], Michel G. Arsenault[1], Chris Riley[3], Michael Kolios[4] and William M. Whelan[1,2]

[1]Department of Physics, University of Prince Edward Island, Charlottetown (Canada)
[2]Department of Biomedical Sciences, Atlantic Veterinary College, Charlottetown (Canada)
[3]Department of Health Management, Atlantic Veterinary College, Charlottetown (Canada)
[4]Department of Physics, Ryerson University, Toronto (Canada)

ABSTRACT

Prostate cancer is currently the most common cancer among Canadian men. Due to an increase in public awareness and screening, prostate cancer is being detected at earlier stages and in much younger men. This is raising the need for better treatment monitoring approaches. Optoacoustic imaging is a new technique that involves exposing tissues to pulsed light and detecting the acoustic waves generated by the tissue. Optoacoustic images of a tumour bearing mouse and an age-matched control were acquired for a 775 nm illumination using a reverse-mode imaging system. A murine model of prostate cancer, TRAMP (transgenetic adenocarcinoma of mouse prostate), was investigated. The results show an increase in optoacoustic signal generated by the tumour compared to that generated by the surrounding tissues with a contrast ratio of 3.5. The dimensions of the tumour in the optoacoustic image agreed with the true tumour dimensions to within 0.5 mm. In this study we show that there are detectable changes in optoacoustic signal strength that arise from the presence of a tumour in the prostate, which demonstrates the potential of optoacoustic imaging for the monitoring of prostate cancer therapy.

Keywords: optoacoustic, imaging, prostate cancer, TRAMP mouse model

1. INTRODUCTION

Optoacoustic (OA) imaging is an experimental clinical imaging technique that involves exposing tissues to pulsed laser light and detecting the acoustic waves generated by the tissues. It is based on the optoacoustic effect whereby short laser pulses absorbed by tissues cause local expansion that leads to the generation of a high frequency pressure wave (ultrasound) which travels outward through the tissue and is detected by transducers that transform the resulting signal into a three-dimensional image of the tissue target [1].

Tissues with higher blood concentrations (for example, solid tumours) experience higher optical absorption which leads to the generation of stronger pressure waves than those generated by surrounding tissues having lower blood concentrations making cancers ideal targets for OA imaging [2].

Prostate cancer is the most common cancer among Canadian men. According to the Canadian Cancer Society, in 2009, an estimated 25,500 men will be diagnosed with prostate cancer and over 4,400 will die of it [3]. Due to an increase in public awareness and screening, prostate cancer is being detected and treated at much earlier stages and in younger men. This is raising the need for better treatments and treatment monitoring approaches. Side effects, even of successful treatments, may include incontinence, impotence and changes in bowel habits [3]. Several new treatments options, including thermal therapy, may offer benefits over current treatments, but the clinical utility is limited due to few treatment monitoring options [4].

In this study, we obtained optoacoustic images of the tumour bearing mice *in vivo* and investigated the capability of optoacoustic imaging to accurately detect the presence and extent of tumours in a mouse prostate adenocarcinoma model.

2. METHOD AND MATERIALS

2.1 Mouse model

The TRAMP (transgenic ardenocarcinoma of mouse prostate) animal model was chosen for this study. The TRAMP mouse develops spontaneous autochthonous prostate cancer with distant site metastasis and can progress to androgen independent disease. This model has been chosen because changes in the TRAMP model mimic those reported in human clinical disease. This model supports the formation of prostate tumours as early as 12 weeks of age, and the cancer may metastasis as early as 24 weeks of age [5].

Furthermore, the TRAMP model can also be used as a potential tool to study mechanisms regarding prostate cancer initiation and progression [6]. Two animals were used in this study, one TRAMP and one control (Jackson Laboratories Inc, Maine, USA), age matched at 24 weeks.

2.2 Optoacoustic detection

Prior to imaging, the animal was placed in an anesthesia induction chamber and anesthetized using isoflurane. Once anesthetized, the hair on the lower abdomen of the animal was removed using a chemical hair remover. The animal was secured to a vertical holder and lowered into a waterbath up to the neck, part of a reverse-mode optoacoustic imaging system (Imagio, Seno Medical, San Antonio, TX, USA). Imaging in water is required for good acoustic coupling.

The imaging system consists of an Nd:YAG pumped Ti:sapphire (775 nm) laser and an 8 element annular array transducer with a central frequency of 4 MHz (Figure 1). A bifurcated optical fiber bundle delivers 6 ns pulses at 775 nm with a 10 Hz repetition rate and 12 mJ pulse energy. Throughout the imaging process, the mouse remains stationary as the fiber bundle and transducer array perform a raster scan across the selected area moving in 0.2 mm steps. Optoacoustic data was acquired from a 15 mm by 10 mm region at the lower abdomen of the mice that included the prostate. The total imaging time was approximately 1.5 hours. Post-imaging, the mice were euthanized and flash frozen in liquid nitrogen. The lower abdomen was dissected out and placed in cryogen. One hundred micron lateral cryosections were acquired.
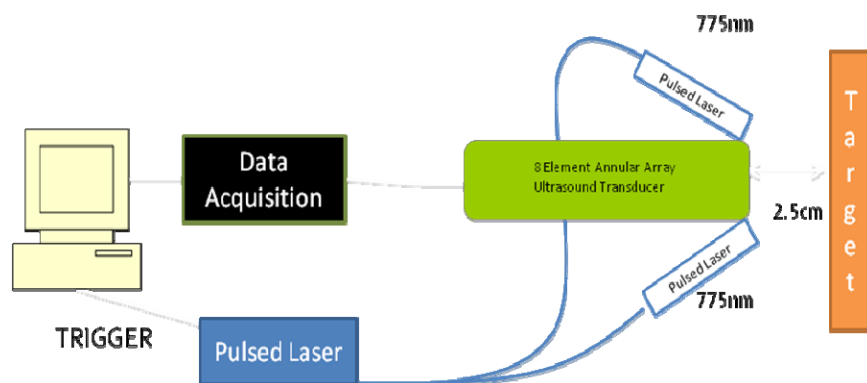

Figure 1: Schematic of the SENO optoacoustic imaging system.

2.3 Data Analysis

All optoacoustic data were exported to Matlab for analysis. The Hilbert transform was applied to all optoacoustic RF data and the signal strength presented has arbitrary units. Due to limited axial resolution of this system, the axial data was compressed to two dimensions to give the optimal coronal prediction of maximum tumour size and position. Only data from a time window corresponding to between 1 mm to 11 mm below the skin surface was used for analysis. This removed the typical strong signals acquired from the animal surface and included only A-line data from tissue regions that included the prostate. The average signal value within each time window was calculated. This value was used as the corresponding pixel value in the final 2-dimensional image.

3. RESULTS AND DISCUSSION

Cryosection images of the prostate region in the TRAMP and control mouse are shown in Figure 2, including the approximate areas imaged on both animals. The cryosection of the TRAMP mouse (Fig 2a) is at 6 mm beneath the surface which corresponds to the maximum lateral tumour dimension. The tumour is clearly visible in the TRAMP mouse and the maximum lateral tumour dimension was determined by visual inspection to be 9.0 ± 0.5 mm. The cryosection of the control mouse shown in Fig 2b is at the same depth as in the TRAMP animal. Averaged optoacoustic images of the prostate region for the TRAMP and control animals are shown in Figures 3 a and b, respectively. The maximum lateral tumour dimension in the optoacoustic image of the TRAMP mouse was determined using the Full Width Half Maximum (FWHM) method to be 9.0 ± 0.5 mm [7]. The uncertainty in this tumour dimension was calculated by varying the FWHM by 10%.
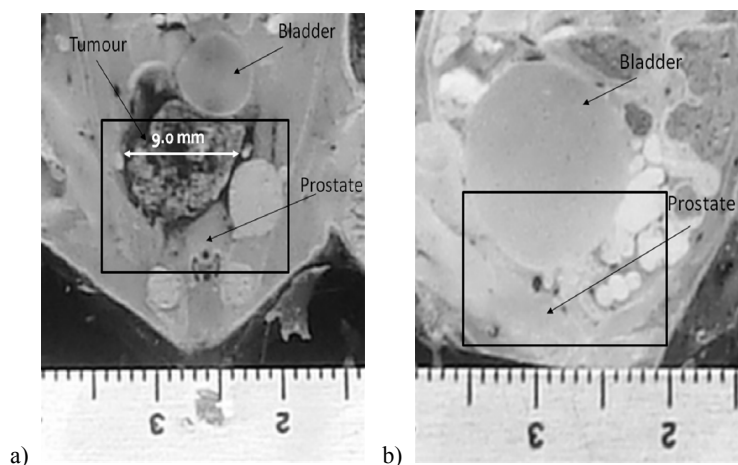

Figure 2: Cryosection Images of (a) TRAMP mouse and (b) control mouse. Imaged area represented by black box (± 1 mm).
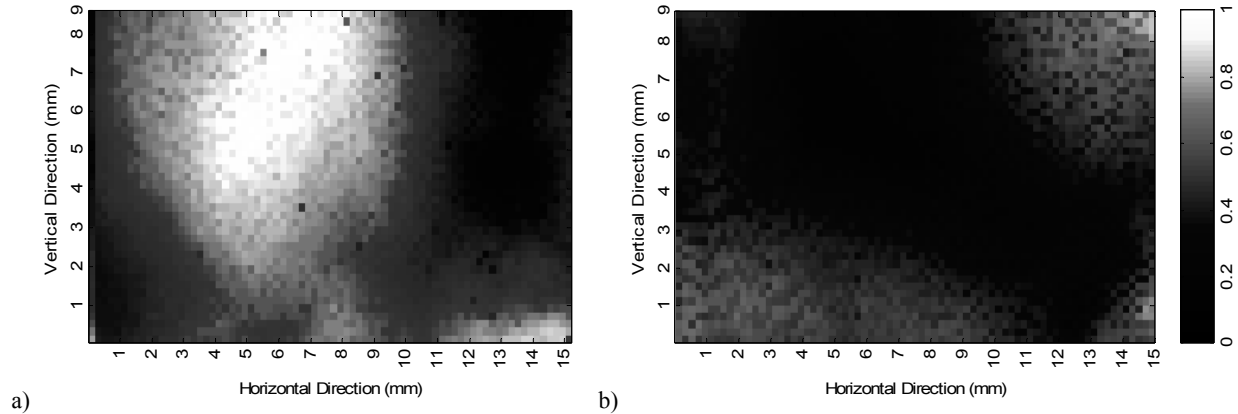
a)   b)

Figure 3: Optoacoustic Images of (a) Tramp mouse with 9 mm tumour, and (b) control mouse with no tumour.

Optoacoustic signals in 2 mm by 2 mm regions of interest centered on the tumour and on the tissue adjacent to the tumour were used to determine a tumour to background contrast ratio which was calculated to be 3.7 ± 0.7. The average contrast ratio for tumour (TRAMP mouse) to normal prostate (control mouse) was determined to be 2.7 ± 1.0.

The TRAMP mouse had no visible indication of tumour growth at the time of imaging (i.e. the tumour did not visibly displace the skin and could not be palpated). This is an important characteristic of the TRAMP mouse as prostate tumours cannot be palpated in the human disease. The imaged region did not cover the full vertical area of the tumour and therefore only the bottom portion of the tumour can be seen in the image (Fig 3a). The dimension in the optoacoustic image horizontally across the tumour agrees with the true dimension of the tumour to within 0.5 mm. We expect similar agreement with the vertical dimension.

4. CONCLUSION

In this study we observed an increase in optoacoustic signal generated by a tumour compared to that generated by the normal prostate or surrounding non-tumour tissues. We also demonstrated excellent agreement between measured tumour dimensions via cryosectioning and predicted tumour dimensions obtained with optoacoustic imaging. Our results demonstrate that optoacoustic imaging may be a suitable candidate for monitoring prostate cancer therapies and merits further investigation.

5. REFERENCES

[1] Xu, M., Wang, L.V., "Photoacoustic imaging in biomedicine," Review of Scientific Instruments 77, 041101 (2006).

[2] Ku, G., Wang, X., Xie, X., Stoica, G. & Wang, L.V, "Imaging of tumor angiogenesis in rat brains in vivo by photoacoustic tomography," Applied Optics 44, 770-775 (2005).

[3] Canadian Cancer Society/National Cancer Institute of Canada, "Canadian Cancer Statistics 2009," Toronto, Canada, 2009.

[4] Larina, I., Larin, K., Esenaliev, R., " Real-time optoacoustic monitoring of temperature in tissue," Journal of Applied Physics 38, 2633-2639 (2005) .

[5] Gingrich, J.R., Barrios, R.J., Foster, B.A., Greenberg, N.M., "Pathologic progression of autochthonous prostate cancer in the TRAMP model," Prostate Cancer and Prostatic Diseases 2, 70-75 (1999).

[6] Shappell, S., Thomas, G., Roberts, R., *et al*, "Prostate pathology of genetically engineered mice: Definitions and classification. The consensus report from the Bar Harbor meeting of the mouse models of human cancer consortium prostate pathology committee," Cancer Research 64, 2270-2305 (2004).

[7] Webb, S., [The physics of medical imaging], Taylor & Francis 33 (1988)